Research Progress in Mechanical and Manufacturing Engineering Vol. 2 No. 2 (2021) 142-150
© Universiti Tun Hussein Onn Malaysia Publisher's Office

RPMME

Homepage: http://publisher.uthm.edu.my/periodicals/index.php/rpmme
e-ISSN : 2773-4765

A Study of Finite Element Analysis For The Thermal Distribution of Friction Stir Welding

Eric King Teck Wee[1], **Rosli Ahmad**[1*]

[1]Faculty of Mechanical and Manufacturing Engineering,
Universiti Tun Hussein Onn Malaysia, 86400 Batu Pahat, Johor, MALAYSIA

*Corresponding Author Designation

DOI: https://doi.org/10.30880/rpmme.2021.02.02.018
Received 02 Aug. 2021; Accepted 27 Nov. 2021; Available online 25 December 2021

Abstract: The Friction Stir Welding (FSW) is a thermal-mechanical, solid state joining technique, which developed into viable technology for the development of sheet and sheet material, including plate materials, for applications in various industries, including plating or plate materials, for use in different industries. This study focused on thermal distribution modeling to better understand thermal distribution during friction stir welding in relation to welding parameters. The key parameters that are taken into account are the rotational speed of the tool and the travel speed. The temperature distribution in the friction stir welding process was simulated using the Finite Element Method (FEM) software, Abaqus Unified FEA. The results show that the higher the tool's rotation speed, the more heat is distributed around the surface of the welding plate. The outcomes of this research provide knowledge of the thermal distribution along the surface of the welding plate using finite element analysis.

Keywords: Friction Stir Welding(FSW), Heat Distribution, Thermal Distribution

1. Introduction

Friction Stir Welding is an advanced technology known as "green" technology because of energy efficiency of the process, environmental friendly and adaptability from the technology [1]. FSW consume less energy during the welding process compared to standard welding methods such as Tungsten Inert Gas (TIG), Arc Welding and so on. In the processes of FSW there is no gas and no flux cover being used where FSW is consider to be an environmental friendly. In the process of joining, there is no metal filler that involves, therefore any alloy can be joined without worrying about the compatibility of the composition, which is a problem in the fusion welding process. Welding by friction stirring can be applied to different types of joints, such as butt joints, lap joints, and etc.

Long before the invention of FSW, a number of significant technological developments in non-fusion welding processes had been established and some limited industrial applications had been identified. A significant process of this is the friction welding that was created just before the laser was invented. During friction welding, the parts to be welded are compressed together made more relative

*Corresponding author: roslee@uthm.edu.my

to each other. As a result, frictional heat is produced to soften the material in the joining area. The last step is to apply an increased pressure to the softened material to create a metallurgical joint without melting the joint material. However the relative movement during the heat generation and material softening process can be basically either rotary or linear. Although the friction welding process is simple, the welding geometry is very restricted and therefore its use is also limited. Generally, one of the basic requirements for the invention of FSW in solid state welding is the thermo mechanical principle of friction welding. The Welding Institute (TWI) in the UK has conducted research and development for years involving the activities of friction welding and surfacing.

There are few variables used to assess the outcome of the welding process. The welding process affects these joint properties mainly through heat generation and diffusion, so that the attention is given to the effect of the welding process variables on heat generation and related outcomes. The motion of the tool produces frictional heat inside the work pieces, extruding the softened plasticized material around it and forging the identical in place to form a solid-state seamless joint [2]. The heat produced at the interface between the tool and the work piece, which is the driving force for the FSW process to be successful [3]. The quantity of heat conducted determines the quality of the weld, deformation, and residual stress in the work piece [4].

2. Materials and Methods

The materials and methods section, otherwise known as methodology, describes how this study was carried out. The goal of this case study and model verification was to identify the FEM model friction stir welding geometry that would be utilized to analyze the heat distribution of friction stir welding. The FEM model was then simulated with the Abaqus program. The system will next analyze the end result in which the heat distribution in the FEM model may be identified. The goal of the parametric study in this study was to investigate the difference in reaction to the FEM model, which the FEM model would test with two types of materials at different rotational speeds of the tool.

2.1 Parameters used In FEM Analysis

For the case study simulation part geometry for the tool, the shoulder diameter was 15 mm, while the pin diameter and length were 5 mm and 4 mm, respectively. Both materials have workpiece dimensions of 130 mm in length, 60 mm in width, and 6 mm in thickness.

Tool selection is a vital aspect of friction stir welding. Tool material characteristics can be critical for FSW. The selection tool material depends on the work piece and the ideal tool life, as well as the user's own experience and expectations. Ideally, the tool material should have the following characteristics:

i. Higher compressive yield strength at elevated temperature than the expected forge forces onto the tool

ii. Good strength, dimensional stability and creep resistance

iii. Good thermal fatigue strength to resist repeated heating and cooling cycles

iv. No harmful reaction with the work piece material

v. Good fracture toughness to resist the damage during plunging and dwelling

vi. Low coefficient of thermal expansion between the probe and the shoulder materials to reduce the thermal stresses

vii. Good machinability to ease manufacture of complex features on the shoulder and probe

Due to the different geometrical characteristics of the tools, the movement of the material around the probe can be extremely complex and significantly different from one tool to the other [5]. The friction stirring probe can cause deformation and frictional heating. It is ideally designed to disrupt the contacting surfaces of the work piece, shear the material in front of the tool and move the material behind the tool. Depth of deformation and tool travel speed are primarily controlled by the probe [6].

2.2 Material Properties

The definition of the material in the FEM analysis is important in order to obtain data on the distribution of heat. Important material definition is the mass density of the material, the Young's modulus, E, the Poisson ratio, v, thermal conductivity, k, and the specific heat of the material, cp. Table 1 show the materials properties that use in the analysis of FEM model.

Table 1: Material properties used in FEM analysis

Material	Mass Density, ρ (T/mm^3)	Young's modulus, **E** (MPa)	Poisson Ratio, *v*	Thermal Conductivity, ***k*** (W/mm °C)	Specific heat, cp (J/T°C)
Steel	7.85e-09	215000	0.29	0.05	468000
Al Alloy	2.64e-09	70000	0.32	0.15	887000
Magnesium Alloy	1.74e-09	42000	0.35	0.16	1024000

It is important to determine the material properties of the FEM model in order to obtain the results of the heat distribution analysis. Material properties can be created by using the material manager in the FEM software, which can determine the material behavior with the appropriate data. The density of the material is set uniformly throughout the material. As far as elastic behavior is concerned, it is important to overcome any permanent change when stress is applied. Thermal conductivity is also one of the important factors for expressing the ability of the materials to conduct heat. Finally, the specific heat capacity is set so that the FEM can measure the amount of heat energy needed to change the material temperature.

2.3 Meshing

Mesh is one component that can have an impact on the outcome because mesh convergence is a critical issue in both Abaqus/Standard and Abaqus/Explicit. Figure 1 shows a few meshes. Because the mesh has fewer elements and the elements are larger in size, the coarse mesh predicts less accurately. The very fine mesh has more elements that can predict more accurately, which can be useful in high stress gradients. The mesh sensitivity analysis was critical in determining an appropriate element size to accurately model the FSW process while incurring the least amount of computational cost [7].

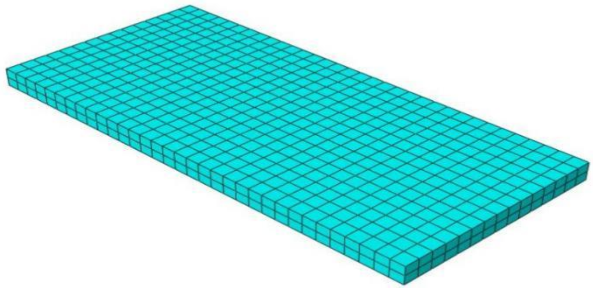

Figure 1a: Coarse mesh

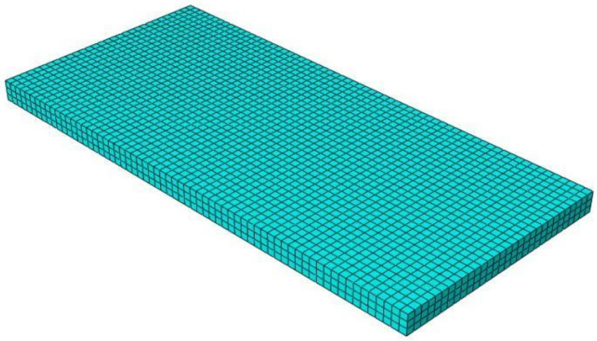

Figure 1b: Fine mesh

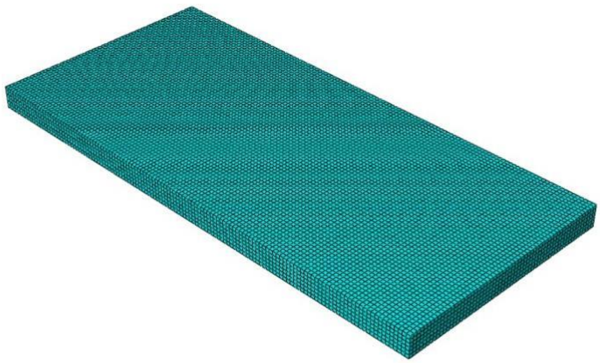

Figure 1c: Very fine mesh

One of the most important steps is to generate the finite element mesh at the mesh stage. The material will be set to explicit with coupled temperature-displacement, and the mesh type must be C3B8T. This is because C3B8T is the correct element for temperature displacement, as shown in Figure 2.

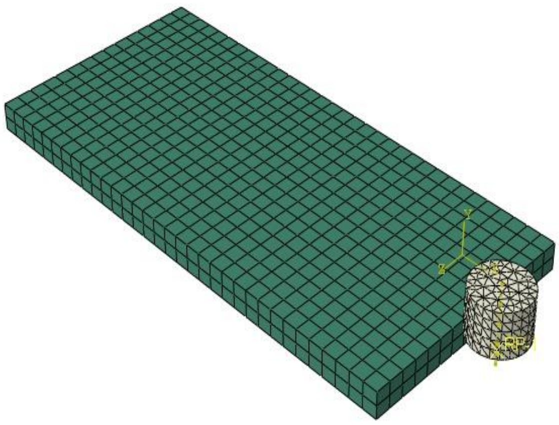

Figure 2: Example of C3B8T Mesh on Workpiece

3. Results and Discussion

The data and analysis from the study are presented in the results and discussion section. Data analysis is the process of analyzing the data obtained in accordance with the study's objectives. The collected results were explained in detail.

NT11 is a temperature output at the section point that can be used in the model to forecast the rate of temperature increase. Throughout this simulation model, boundary conditions were established in Abaqus Software in FSW. For example, in order to obtain the temperature distribution in the welded plates during the friction stir welding operation, the tool's rotating speed can be 600 rpm, 800 rpm, or 1000 rpm with a travel speed of 10 mm/s. The results of this investigation will only focus on the surface temperature of the materials.

3.1 Temperature reading for AI alloy and Mg alloy

Each temperature reading for AI alloy and Mg alloy will be estimate taken from the start of surface contact, in the middle of the process, and at the end of the process. All of the results are gathered at all three rotational speeds of 600rpm, 800rpm, and 1000rpm.

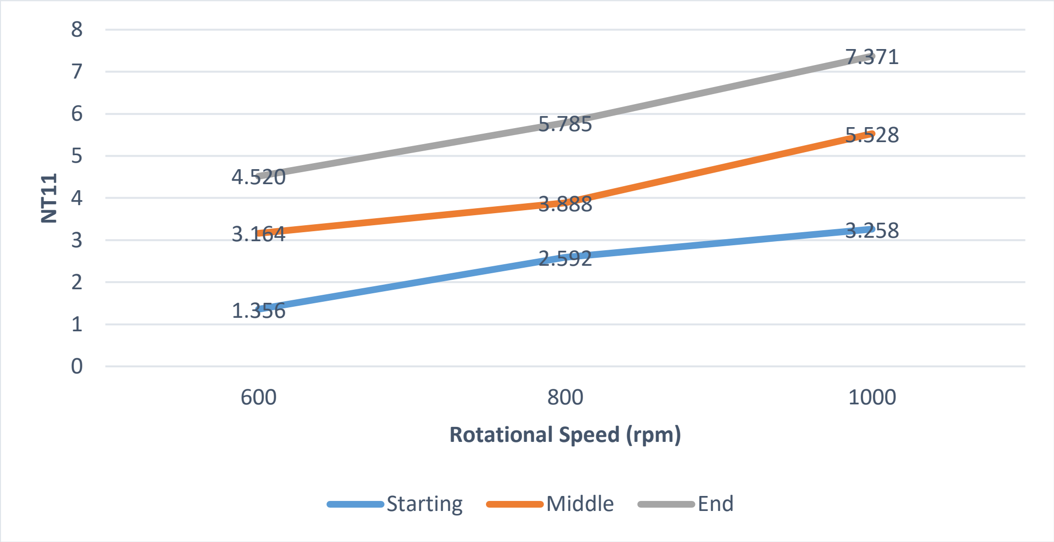

Figure 3: NT11 result on AI_Alloy Plate

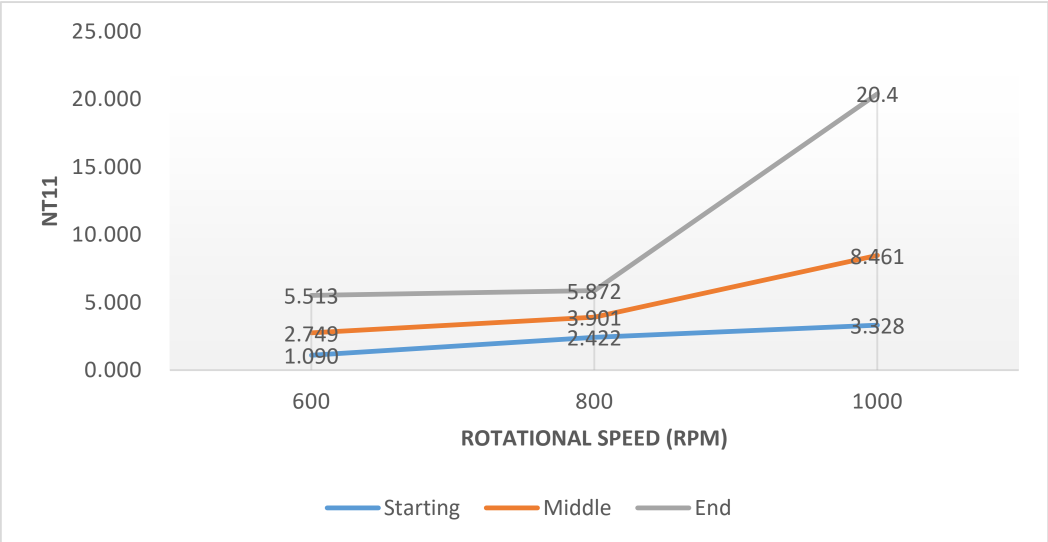

Figure 4: NT11 result on Mg_Alloy Plate

Figures 3 and 4 show the NT11 results obtained from the finite element simulation. As a result, it is possible to see that as the rotational speed increases, so does the amount of heat created on the workpiece's surface. The difference can be seen in the final temperature of the work piece, where AI Alloy had an NT11 reading of 4.520 at 600rpm and 7.371 at 1000rpm. The same is true for Mg Alloy, where the NT11 end part reading was 5.513 at 600 rpm and 20.44 at 1000 rpm.

3.2 Differences NT11 for AI alloy and Mg alloy

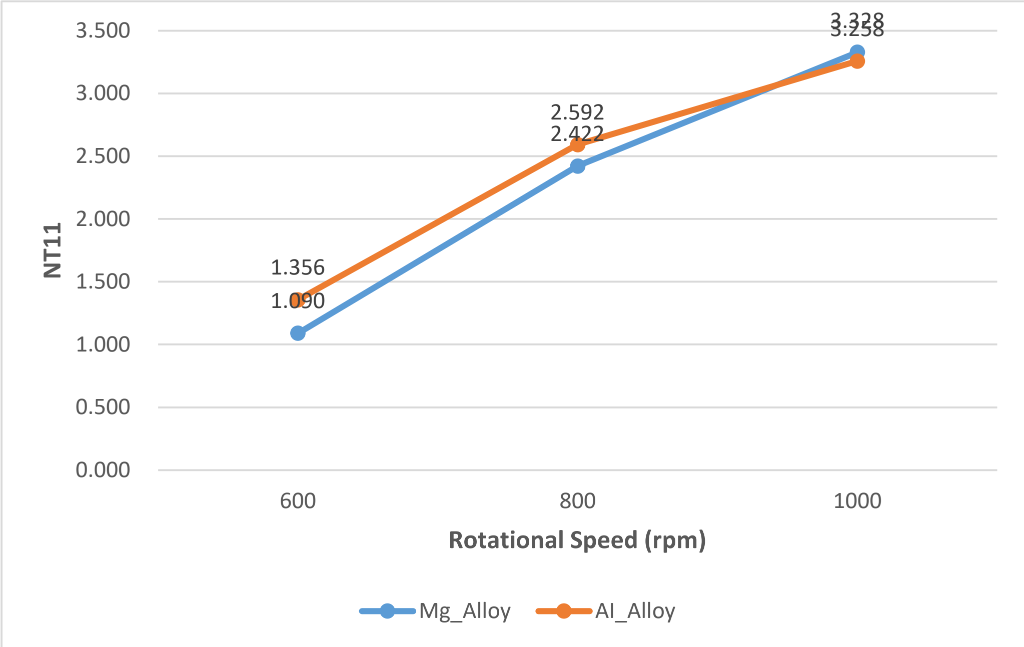

Figure 5: Differences NT11 at beginning

Figure 5 shows that the results for AI alloy and Mg alloy are nearly identical at the start of the process. At 600rpm, the NT11 value is roughly 1.0-1.4. The NT11 increases to roughly 2.4-2.6 at 800rpm. Finally, at 1000rpm, the NT11 continues to rise above 3.0.

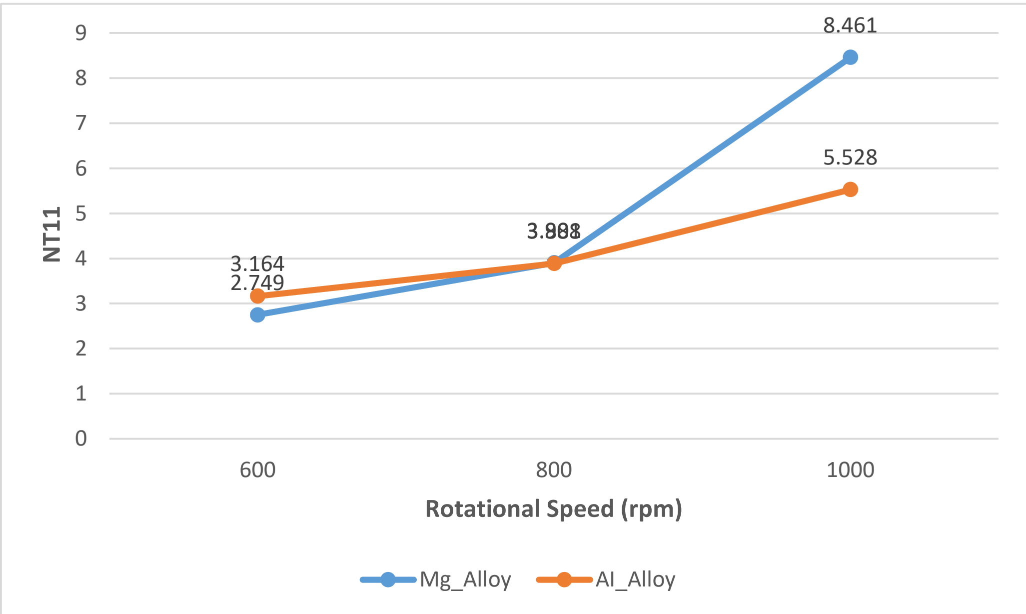

Figure 6: Differences NT11 at mid

The results of the process in the mid of FSW are shown in Figure 6 for both AI alloy and Mg alloy. At 600rpm, the NT11 of AI alloy is slightly higher than that of Mg alloy. At 800 rpm, both materials show nearly identical values: NT11 AI alloy is 3.888 and Mg alloy is 3.901. However, at 1000rpm, NT11for Mg alloy increases faster than AI alloy

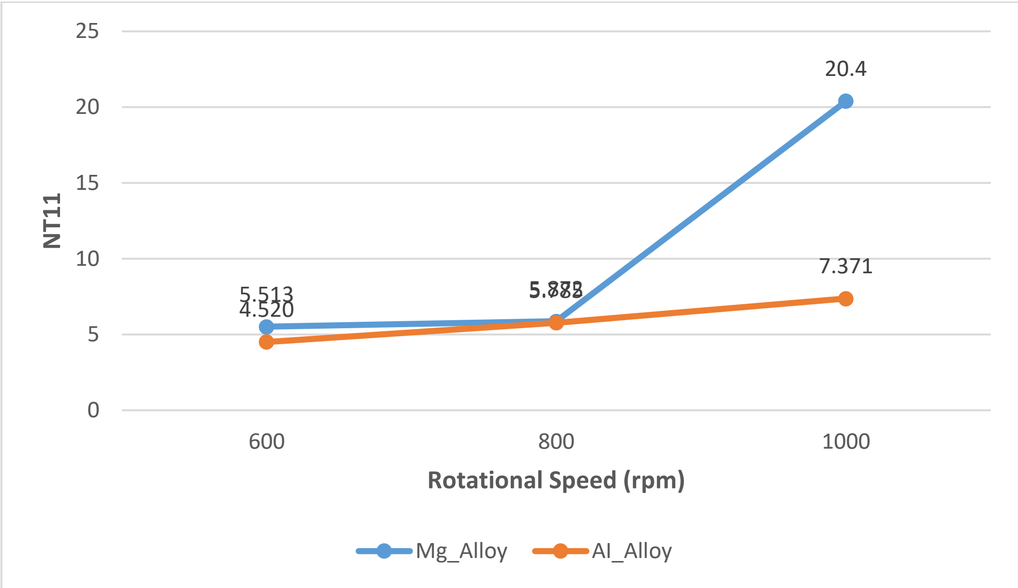

Figure 7: Differences NT11 at end

Figure 7 depicts the difference in results obtained for Al alloy and Mg alloy at the end of the process. At 600rpm, both materials exhibit a high NT11 when compared to the beginning and middle of the process. At 600 rpm, the NT11 ranges from 4-5.6. The NT11 for both materials increases slightly about 5 over 800 rpm. At 1000 rpm, it shows a significant rise in NT11 for Mg alloy. This is because to the high thermal conductivity of Mg alloy. Thermal conductivity a material's capacity to conduct heat. High thermal conductivity materials may effectively transfer heat and rapidly absorb heat from their surroundings. Poor thermal conductors obstruct heat flow and provide heat slowly.

3.3 Discussion and review

Based on the information obtained, it can be determined if Mg alloy and AI alloy materials should be joined. AI alloy must be used on the advancing side, and Mg alloy on the retreating side. This is because, according to the data, Mg alloy generates heat faster than AI alloy. That is why the AI alloy must be on the advancing side so that the Mg alloy does not completely melt during the process. Even with the obtained results, it is crucial to note that the accuracy of the results reported in this study is limited.

The experiments of E.E.M. KISHTA et al. [7] demonstrate a different thermal profile for the friction stir process. Various rotational speeds will generate different results. The different temperatures on the surface of the work piece can be seen perfectly with a find mesh. The Adaptive Eulerian Lagrangian (ALE) meshing technique, which is critical for large deformation modeling, was also used to avoid element distortions during the process. A percentage of material is specified to fill each element when employing Eulerian elements. The ALE approach allows the elements to begin with 100 percent material and gradually change the percentage of material per element as the process progresses, allowing the material to stir without generating distortions or artificial voids [8]. (Hofmann D.C,2005)

The Lagrangian approach is primarily used in conjunction with solid and structural elements. In the case of FSW, the Lagrangian approach can produce correct global findings. As previously stated, the nodes in this approach move with the material and follow its deformation. As a result, there are no material transfers between elements in this method, making it suited for analyzing processes where the mesh distribution is not large (outside of the welding zone) [9] [10].

4. Conclusion

To summarize, this research focuses on the temperature distribution over the surface of a workpiece with varying rotational speed. It was discovered that conducting the simulation with a limited understanding of the FEM program is difficult. The friction stir welding finite element technique was successfully completed. Due to a lack of understanding of the FEM, a few errors arise when performing meshing on the tool, resulting in element distortion when the simulation runs. This is because the mesh has been configured wrongly. Aside from that, although utilizing fine mesh can help to solve the FEM and produce a better result, it will take significantly longer time for the simulation. However, there is still room for development in order to achieve a better outcome for this study.

Acknowledgement

The authors would like to thank the Faculty of Mechanical and Manufacturing Engineering, Universiti Tun Hussein Onn Malaysia for giving the opportunity to conduct this study.

References

[1] R.S Mishra, Z.Y.Ma, Friction stir welding and processing, Materials Science and Engineering R 50 (2005)

[2] Xunhonga Wang, Kuaishe Wang, Microstructure and properties of friction stir butt-welded AZ31 magnesium alloy, Materials Science and Engineering A 431 (2006)

[3] Prasanna Kutum, Manash Jyoti Borah. Experimental analysis on friction stir welding process parameters on temperature distribution. Indian Journal of Engineering, 2016, 13(33), 394-400

[4] Chao, Y. J., Qi, X., & Tang, W. (2003). Heat Transfer in Friction Stir Welding-Experimental and Numerical Studies. Journal of Manufacturing Science and Engineering, 125(1), 138–145.

[5] Zhang, Y. N., Cao, X., Larose, S., & Wanjara, P. (2012). Review of tools for friction stir welding and processing. Canadian Metallurgical Quarterly, 51(3), 250–261.

[6] W. M. Thomas, E. D. Nicholas, J. C. Needham, M. G. Murch, P. Temple-Smith and C. J. Dawes: GB Patent no. 9125978?8, 199

[7] Kishta, E. E. M., Abed, F. H., & Darras, B. M. (2014). Nonlinear finite element simulation of friction stir processing of marine grade 5083 aluminum alloy. Engineering Transactions, 62(4), 313–328.

[8] Hofmann D.C., Vecchio K.S., Submerged friction stir processing (SFSP): An improved method for creating ultra-fine-grained bulk materials, Materials Science and Engineering, A402, 234–241, 2005

[9] Fu, L.; Duan, L.; Du, S. Numerical simulation of inertia friction welding process by finite element method. Weld. J. 2003, 82, 65–70.

[10] Ghanimi, Y.; Cerjak, H.; Faes, K. Modelling of Friction Welding of Long Components. In Trends in Welding Research: Proceedings of the 6th International Conference, Callaway Gardens Resort, Phoenix, Arizona, 15–19 April 2002; David, S.A., Ed.; ASM International: Geauga County, OH, USA, 2002.